

Electrochemical Preparation and Characterization of Ni–PTFE Composite Coatings from a Non-Aqueous Solution Without Additives

Yi-Hui You, Chang-Dong Gu^{*}, Xiu-Li Wang, and Jiang-Ping Tu

State Key Laboratory of Silicon Materials, Key Laboratory of Advanced Materials and Applications for Batteries of Zhejiang Province, and Department of Materials Science and Engineering, Zhejiang University, Hangzhou 310027, China

*E-mail: changdong_gu@hotmail.com

Received: 10 October 2012 / Accepted: 31 October 2012 / Published: 1 December 2012

Electrodeposition process of Ni–polytetrafluoroethylene (PTFE) composite coatings is limited to use aqueous plating bath where nonionic/cationic wetting agents usually are necessary to prohibit the hydrophobic PTFE particles being coagulated. This study proposes a novel electrolyte for the depositing Ni–PTFE composite coatings which is formed in a deep eutectic solvent (DES). The DES with a non-aqueous nature allows the PTFE particles well be dispersed in the electrolyte without the additive of any wetting agents. The Ni–PTFE composite coatings are successfully electrodeposited from the proposed DES-based plating bath which is confirmed by the scanning electron microscope and X-ray energy dispersive spectroscopy. Deposition mechanism, microstructure, and properties of the composite coatings are investigated. Importantly, it is found that the Ni–3.1wt.% PTFE composite coating shows a hydrophobic behavior with a contact angle of about $121\pm 1^\circ$ and an enhanced wear resistance than the pure Ni coating due to the incorporation of PTFE.

Keywords: Electrodeposition; Ni–PTFE composite; Cyclic voltammetry; Deep Eutectic Solvent; Friction coefficient

1. INTRODUCTION

Metal matrix composite coatings obtained by chemical or electrochemical codeposition techniques have been attracting keen interest during last several decades. The composite electrodeposition consists of the electrolysis of plating solutions in which micron- or submicron size particles are suspended, which enables the production of a wide range of composite materials with improved properties in terms of wear resistance, lubrication or corrosion resistance [1-8]. Different metals are used as matrix and many types of particles, such as ceramics (Al_2O_3 [9, 10], ZrO_2 [11, 12],

SiC [13-17] and polymers (polytetrafluoroethylene (PTFE) [18-22], can be added to improve mechanical and physicochemical properties of the material. Amongst them, Ni-PTFE (polytetrafluoroethylene) composite coatings prepared by electrodeposition method are of particular interest for their good water repellency and solid lubrication due to their low surface free energy and friction coefficient. However, PTFE particles readily coagulate and precipitate in the aqueous Ni plating solution since PTFE is a water-repellent material [19, 23], which will not only reduce the PTFE content in the coatings, but also increase the surface roughness as larger PTFE particles are incorporated [24, 25]. Therefore, much effort has been devoted for developing effective strategies to make the PTFE particles being distributed in the aqueous Ni plating baths. For example, the dispersion of PTFE particles can be stabilized using ultrasonic stirring [22] and nonionic/cationic wetting agents [19, 26-28].

Room temperature ionic liquids (RTILs) are more advantageous media for the electrodeposition of metals and composites due to their wide electrochemical windows and extremely low vapor pressures [29, 30]. More importantly, RTILs generally contain organic groups having the lower surface energy than water, which would be beneficial for the wetting of PTFE particles and dispersion of the PTFE particles in it. Therefore, it would be promising to plate Ni-PTFE composite coatings from the RTIL-based electrolytes without an addition of wetting agents. Deep eutectic solvent (DES) is a relatively new class of ionic liquid based on eutectic mixtures of choline chloride (ChCl) with a hydrogen bond donor species, which was introduced by Abbott and co-workers [31]. Recently, we have demonstrated that Ag [32], Ni [33, 34], porous Sn [35], Ni-Co [36] and Ni-P [37] alloy could be facilely electrodeposited from the ChCl-ethylene glycol (EG) based DES (also known as Ethaline), which indicates the electrochemical deposition from the Ethaline-based electrolytes is an effective method to control the surface morphology of the deposit. Moreover, suspensions of various particulate materials including Si_3N_4 , SiC, BN, Al_2O_3 , and diamond can be formulated simply by stirring the powder solid with the ionic liquid (DES). A key advantage of DESs for this application is that the particulate suspensions are stable over a prolonged period of time; this is presumably due to a combination of the increased viscosity (of the neat liquid), compared to water and the coulombic screening of surface charge by the ionic liquid (high ionic strength) [10].

Abbott et al. have demonstrated that the electrolytic deposition of silver from a solution of AgCl in the Ethaline containing SiC or Al_2O_3 particles could deliver an improved wear resistant silver composite film [38]. Recently, Abbott's group has done a pioneering work on the electrodeposition of Ni-PTFE composite coatings from the DES based electrolytes [39]. They demonstrated that the Ni-PTFE composite coating could be electrodeposited from Ethaline with presence of ethylene diamine as brightener and 1 wt. % LiF [39]. However, their work provided limited information on the deposition process and characterization of the novel Ni-PTFE composite coating. Based on this thought, this study aims to investigate the electrodeposition process of the Ni-PTFE composite coatings from the Ethaline containing PTFE particles. It is worthy of being noticed that no additives or wetting agents were used in this electrodeposition process. Moreover, the microstructure and wear properties of the Ni-PTFE composite coatings were characterized in details.

2. EXPERIMENTAL DETAILS

ChCl and EG were used as received (AR, Aladdin). Ethaline was formed by stirring the mixture of the two components in a mol ratio of 1 ChCl : 2 EG at 80 °C for about 30 min. Many studies had demonstrated that Ni coatings could be electrodeposited from the Ethaline containing $\text{NiCl}_2 \cdot 6\text{H}_2\text{O}$ [34, 36, 40]. In this case, PTFE (AR, Aladdin) particles with a size of approximately 2 μm were added in the Ethaline-based Ni plating bath for the electrodeposition of Ni-PTFE composite coatings. The Ni plating bath contains 1.0 M $\text{NiCl}_2 \cdot 6\text{H}_2\text{O}$ in Ethaline. Two Ni-PTFE plating baths were formed by adding 5 and 10 g l^{-1} PTFE into the Ni plating bath, which would hereafter be denoted as Ni-5PTFE and Ni-10PTFE, respectively. The anode was nickel plate and the cathode was the polished brass substrate. The Ni and Ni-PTFE composite coatings were electrodeposited from the above electrolyte baths at a constant voltage of 1.0 V and room temperature (RT, $30 \pm 2^\circ\text{C}$) for about 2 hour using an agitation velocity of 100 rpm on a magnetic stirrer (IKA[®] RET basic). At last the newly obtained deposits were sequentially rinsed with methanol and deionized water.

A field emission scanning electron microscope (FE-SEM) was used to observe the surface morphology. Chemical composition was analyzed with an X-ray energy dispersive spectroscope (EDS, BRUKER AXS) attached to the SEM. Crystalline structure was studied by X-ray diffractometer (XRD, Rigaku D/max 2550PC) with a Cu target ($\lambda = 1.54056 \text{ \AA}$) and a monochromator at 40 kV and 250 mA with the scanning rate and step being $4^\circ/\text{min}$ and 0.02° , respectively. The surface imaging was performed by atomic force microscopy (AFM, Veeco, Dimension[®] EdgeTM) in a contact mode, from which the surface roughness could be determined.

The static contact angle (CA) measurements were performed by using a commercial instrument (SL200B, Solon Tech., Shanghai). The indicator drop images were stored via a monochrome video camera by using a PC-based control acquisition and data process. Deionized water or Ethaline droplets each having a volume of 1 μL were used in the wetting tests. Cyclic voltammetry and electrochemical measurements for corrosion tests were performed on a CHI604b electrochemical workstation (Chenhua, Shanghai) at room temperature. Cyclic voltammetry experiment was carried out in a three electrode system consisting of a platinum microelectrode (1.1 cm^2), a platinum counter electrode and a silver wire quasi-reference electrode. The cyclic voltammetry experiment was performed at ambient temperature ($30 \pm 2^\circ\text{C}$) and at a scan rate of 1 mV s^{-1} with a stirring rate of 100 rpm in order to make the PTFE particles well dispersed. Linear sweep voltammetry experiments were carried out in a 3.0 wt.% NaCl aqueous solution using a classic three-electrode cell with a platinum plate as counter electrode and a saturated calomel electrode (SCE, + 245 mV vs SHE) as reference. The exposed area of the coatings for testing was obtained by insulated epoxy resin coatings leaving an uncovered area of approximately 1 cm^2 . Before the potentiodynamic sweep experiments, the samples were first immersed into 3 wt.% NaCl solution for about 200 s to stabilize the open-circuit potential. Potentiodynamic curves were recorded by sweeping the electrode potential from a value of about 200 mV lower to a value of 300-500 mV greater than the corrosion potential, at a sweeping rate of 1 mV/s.

The tribological properties of the coatings were performed on a SFT-2M ball-on-disk tribometer. Si_3N_4 ceramic ball (4 mm in diameter, hardness HV=1550) was used as the counter body. The tests were carried out at a normal load of 1 N at a rotational velocity of 300 rpm. The friction

coefficient was monitored continuously during the experiments by a linear variable displacement transducer and recorded on a data acquisition computer attached to the tribometer. Test duration was up to 9000 cycles and the wear tracks were observed by SEM.

3. RESULTS AND DISCUSSION

3.1. Dispersion and suspension of PTFE in Ethaline

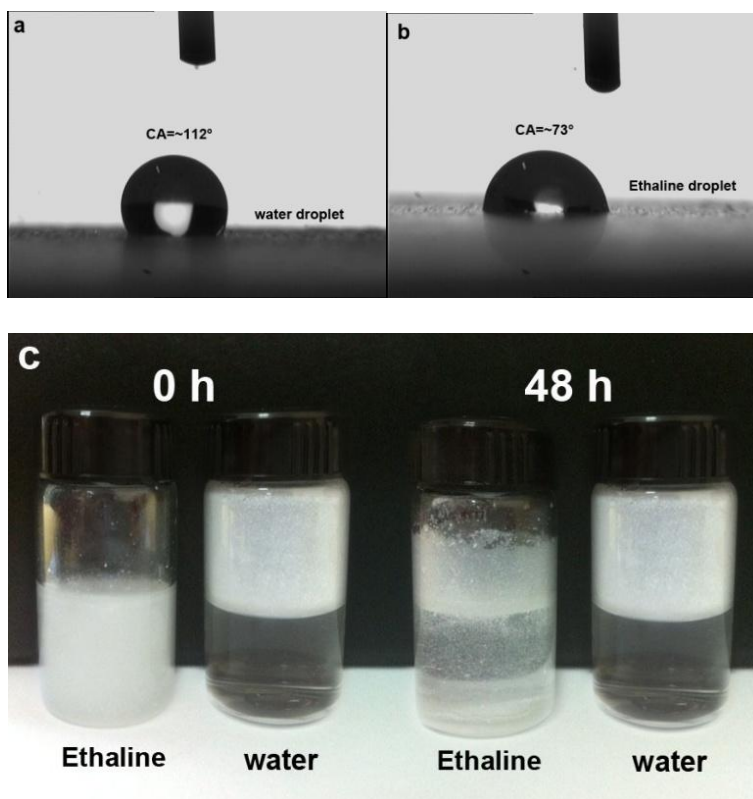


Figure 1. Contact angle measurements of water (a) and Ethaline droplets (b) deposited on the PTFE plate surface and photographs of the PTFE particles in water and Ethaline for 48 h (c).

To evaluate the dispersive ability of PTFE particles in Ethaline, the contact angles (CAs) of the water and Ethaline droplets deposited on a PTFE plate surface were measured, which are shown in Figure 1a and b, respectively. It can be seen that the CA value of water droplet is about 112° while the value of Ethaline droplet is 73°, which indicates that a better dispersion of the PTFE particles would be obtained in Ethaline than in water. Figure 1c shows the stability of PTFE particles dispersed in Ethaline and water, respectively. It is found that the PTFE particles can be well dispersed in Ethaline after a vigorous stirring process. However, the PTFE particles cannot be wetted by the water solvent, as shown in Figure 1c. After the PTFE particles dispersed in Ethaline stewing for about 48 hours at room temperature, the separation of PTFE particles from Ethaline is observed. But, traces of PTFE particles can also be found in the bottom Ethaline. The excellent wettability of PTFE in Ethaline

should be attributed to the organic nature of the solvent and the coulombic screening of particle surface charge induced by the ionic liquid [10]. Therefore, it is possible that Ethaline can be used as a substitution for water to form the novel electrolyte without wetting agents or additives for the electrodeposition Ni–PTFE composite coatings.

3.2. Cyclic voltammetry measurements

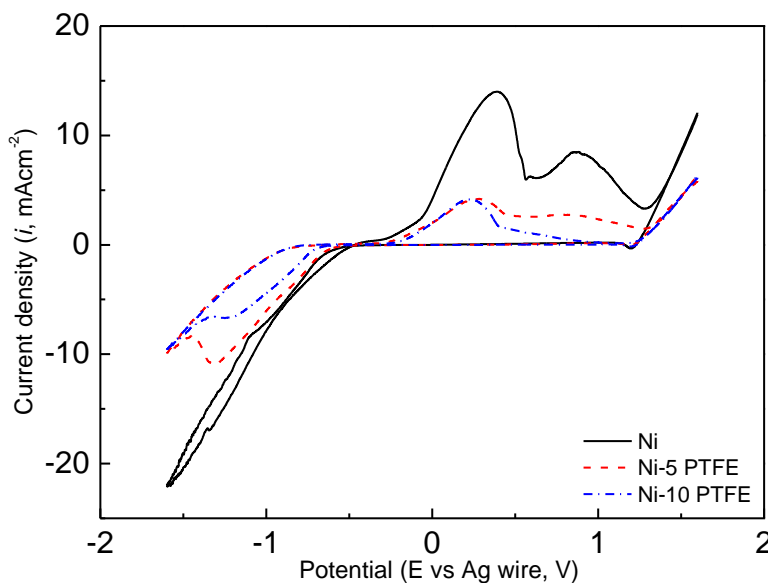


Figure 2. Cyclic voltammograms of the Ni and Ni–PTFE plating electrolytes performed at room temperature and 1 mV/s.

Typical cyclic voltammograms for the Ni plating bath and two Ni–PTFE plating baths are shown in Figure 2. Cyclic voltammograms of Figure 2 exhibit the same general feature: In the cathodic branch a nucleation loop is recorded indicating that bulk deposition of Ni and Ni–PTFE composite coatings requires a significant overpotential to initiate nucleation and growth. For the voltammogram of the Ni plating bath, a small cathodic reduction peak at about -1.340 V and two consecutive oxidation peaks are apparently observed. The onset potential of the reduction of Ni^{2+} is about -0.510 V. As shown in Figure 2, the Ni electrolyte presents a characteristic crossover between the currents for the positive and negative sweeps at the potential of about -0.480 V, which suggests the presence of a nucleation and growth process [41]. The stripping process goes through two consecutive oxidation processes corresponding to the Ni to Ni^+ and Ni^+ to Ni^{2+} . For the Ni–5PTFE and Ni–10PTFE electrolytes, the onset potentials of deposition shift to more negative values of -0.530 V and -0.626 V, respectively. The deposition current density gets smaller than the Ni electrolyte as the content of PTFE increases in the electrolytes, which means the presence of PTFE in the electrolyte inhibits the reduction of Ni ions. The stripping process is also different from the Ni electrolyte and the oxidation peak of Ni^+ to Ni^{2+} gets smaller and disappears for the Ni–10PTFE electrolyte. Therefore, the presence of PTFE in the Ni plating bath alters both the reduction and stripping processes. The difference in cyclic voltammograms should account for the different morphologies of the coatings which are confirmed by the following SEM observations.

3.3. Surface morphology and chemical composition

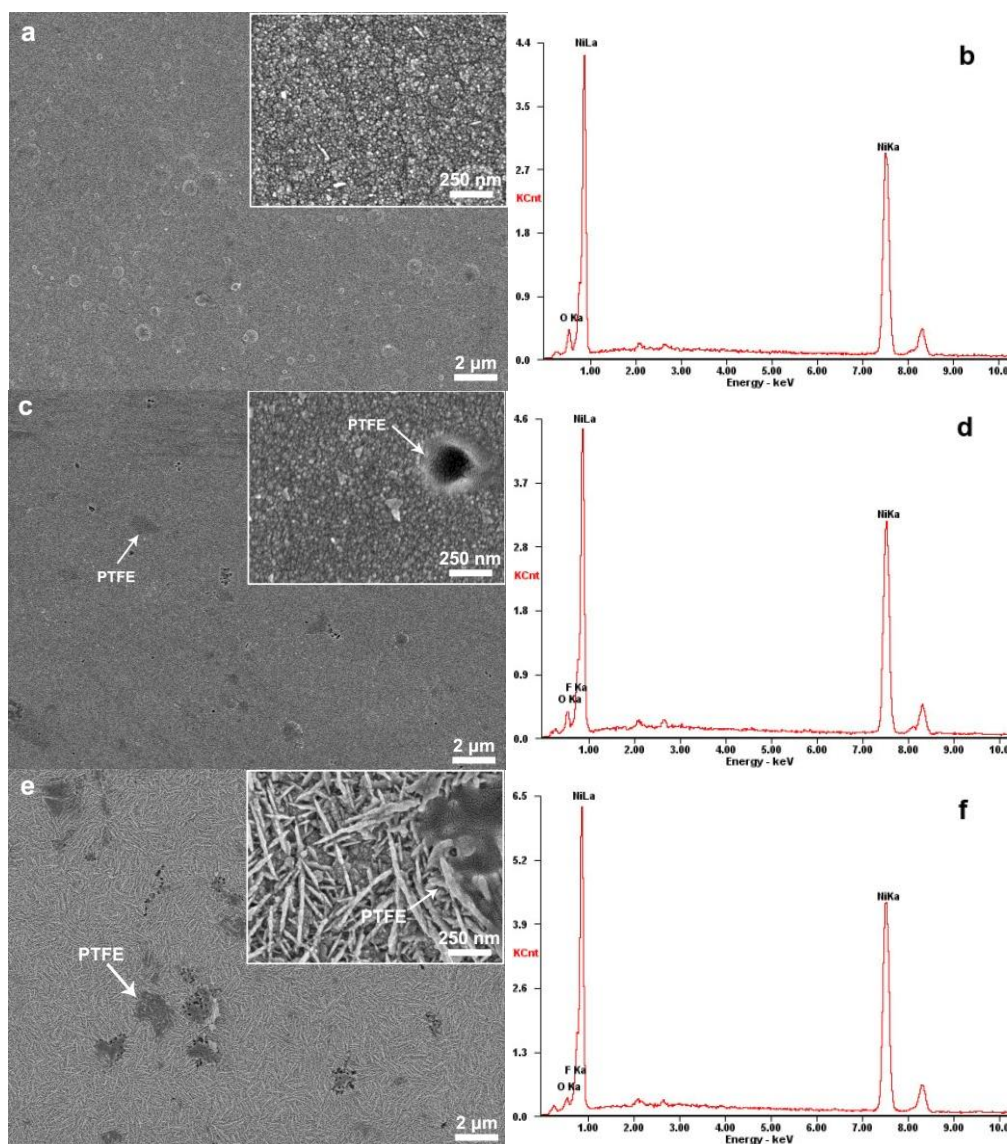


Figure 3. Surface morphologies and corresponding EDS analyses of the electrodeposited Ni coating and Ni-PTFE composite coatings. (a–b): Ni; (c–d): Ni–2.8 wt.% PTFE; (e–f): Ni–3.1 wt.% PTFE, where insets are the corresponding SEM images with high magnification.

Figure 3 shows the SEM images of the pure Ni and Ni-PTFE composite coatings, where the insets are the corresponding SEM images with a high magnification. As shown in Figure 3a, the as-deposited Ni coating from the 1.0 mol l^{-1} $\text{NiCl}_2 \cdot 6\text{H}_2\text{O}$ dissolved Ethaline exhibits a smooth and compact surface, which is in consistency with our previous work [33, 34]. The grains with size of about 10 nm are uniformly distributed in the Ni coating. Some clusters composed of these nano-sized grains can also be observed from the inset of Figure 3a. As shown in Figure 3c, the morphology of composite coating is not significantly changed from the Ni-5PTFE bath. However, PTFE particles can be clearly found in the magnified SEM image (Figure 3c inset), which means that the Ni-PTFE composite coating has been successfully fabricated from the novel electrolyte. Figure 3e gives the

surface morphology of the Ni-PTFE composite coating electrodeposited from the Ni-10PTFE bath, which is largely different from the pure Ni and Ni-5PTFE coatings, but similar to that of the Ni coating electrodeposited at a high temperature of 90 °C [34]. The surface is composed of plenty of needle-like rods which are randomly distributed and the PTFE particles are embedded into these rods. Each needle-like rod with a diameter of about 20-30 nm is composed by numerous aligned Ni strips with the length of about 200-500 nm and the thickness of less than 20 nm. Therefore, the presence of PTFE particles in the Ni plating bath has a significant effect on the surface morphology of the composite coatings. However, the mechanism underlying the effects should be attributed to the nucleation and growth process revealed by cyclic voltammograms.

The EDS analysis gives the composition of Ni and Ni-PTFE composite coatings. For pure Ni, the coating is mainly composed of Ni (96.54 wt.%). According to the chemical formula of PTFE, the content of F in the PTFE material is known. The F content in the coating can be measured by the EDS analysis. Therefore, the content of PTFE in the composite coating can be approximately calculated. The contents of PTFE in the two composite coatings electrodeposited from the electrolytes of Ni-5PTFE and Ni-10PTFE are 2.8 wt.% and 3.1 wt.%, respectively. It can be found that the PTFE content in the composite coatings increases a little as the concentration of PTFE increases in the electrolytes. It is also found that there is small amount of O existing in the coating, which might be from the environment.

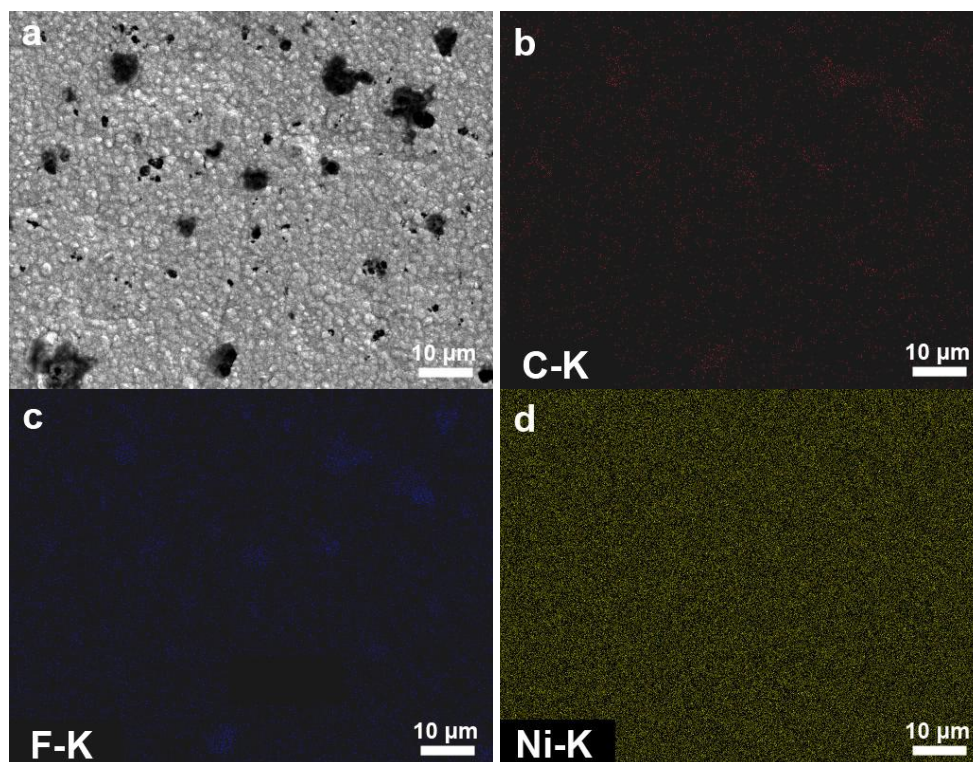


Figure 4. (a) SEM image of the Ni-3.1 wt.% PTFE composite coating for the EDS mapping analysis. The corresponding elemental mapping images for C, F, and Ni are presented in (b), (c), and (d), respectively.

As a representative case of study on the distribution of PTFE particles in the composite coatings, the element distribution revealed by EDS mapping was carried out on the Ni–3.1 wt.% PTFE composite coating, which is given in Figure 4 where (a) is the SEM image and (b)–(d) presents the C, F, and Ni mappings, respectively. As expected, the C and F signal are very strong in the position of the particles. The intensity of Ni is strong all around the surface. The result further confirms that the PTFE particles have been successfully incorporated into the Ni matrix which is in agreement with the result shown by K.E. ttaib [39].

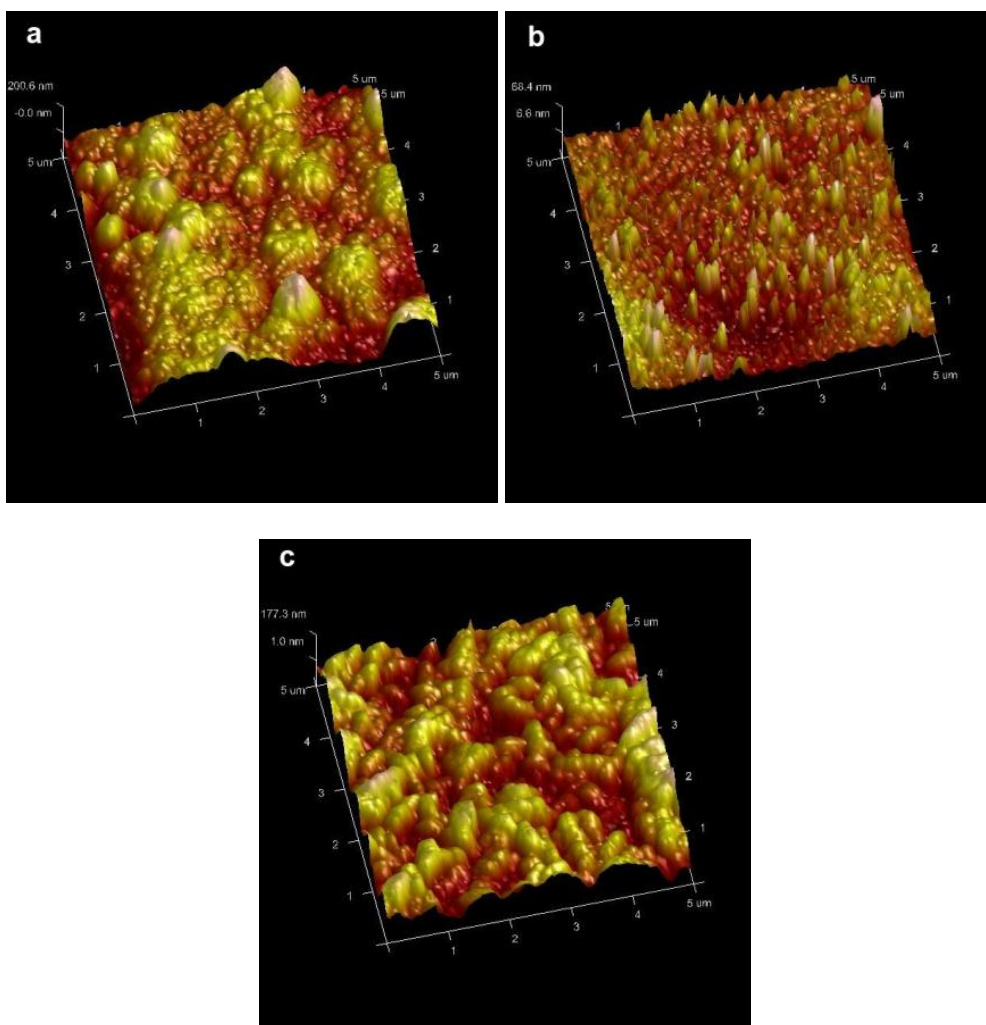


Figure 5. Typical three-dimensional AFM images ($5\ \mu\text{m} \times 5\ \mu\text{m}$) of the electrodeposited Ni coating and Ni–PTFE composite coatings. (a): Ni; (b): Ni–2.8 wt.% PTFE; and (c): Ni–3.1 wt.% PTFE.

Surface topography and roughness can be characterized by AFM [21]. Figure 5 shows representative AFM images ($5\ \mu\text{m} \times 5\ \mu\text{m}$ in size) corresponding to the surface topography of the Ni and the two Ni–PTFE composite coatings. Clearly, grain clusters with the size range of 10–40 nm are observed on the surface of all the three coatings. Moreover, the pure Ni coating has larger grain colonies than the Ni–PTFE composite coatings, which has an average surface roughness (R_a) of about 41.5 nm. Compared with the Ni coating, the Ni–2.8 wt.% PTFE composite coating has a smooth

surface with Ra of ~ 9.2 nm. However, the surface roughness of the Ni–3.1 wt.% PTFE composite coating increases to ~ 40.0 nm, which is in agreement with the SEM observation as shown in Figure 3e.

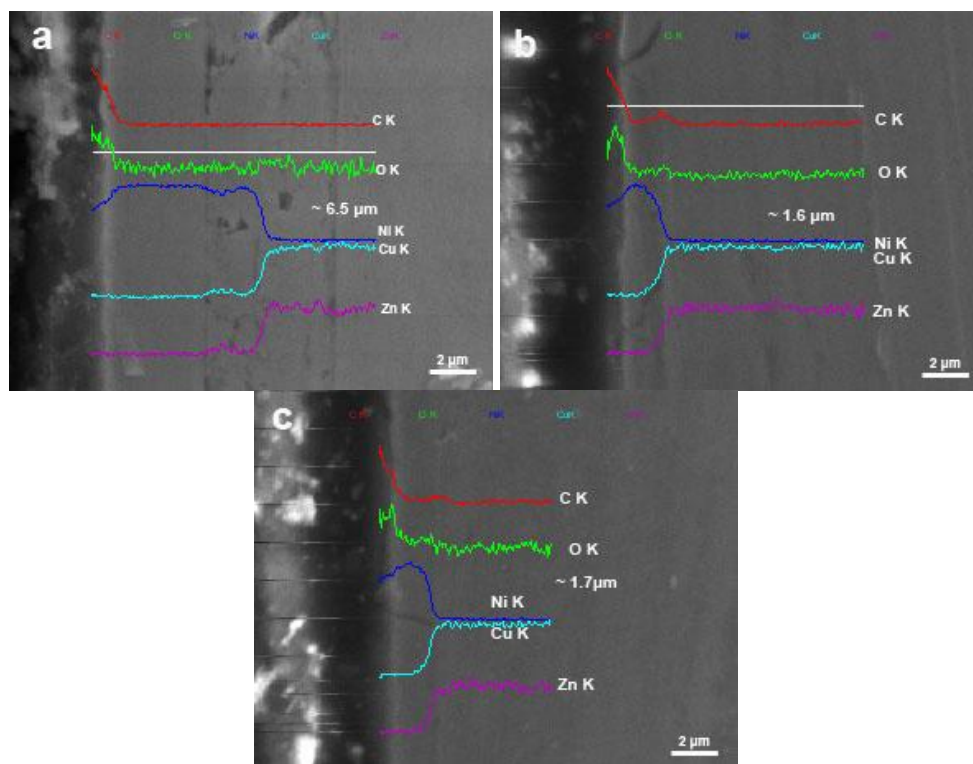


Figure 6. SEM micrograph and EDS linear analysis of the cross-section of electrodeposited Ni and Ni–PTFE composite coatings on brass substrates. (a): Ni; (b): Ni–2.8 wt.% PTFE; and (c): Ni–3.1 wt.% PTFE.

Figure 6 shows the SEM images incorporated with EDS linear analyses of the cross-section of electrodeposited coatings. It is hard to distinguish the coating/substrate interface in the SEM images, which implies that the coatings are well coherent to the substrate. With the aid of EDS linear analysis as shown in Figure 6, the thickness of coatings can be easily distinguished [36]. The EDS signals of C and O shown in Figure 6 mainly come from the epoxy resin and the Cu and Zn are originated from the brass substrate. The EDS liner profile of F originated from PTFE is not shown in Figure 6b and c because of the low PTFE content in the composite coatings. The pure Ni coating has a thickness of about $6.5 \mu\text{m}$ (Figure 6a). However, the thickness of the two Ni–PTFE coatings is about $1.6 \mu\text{m}$, which is much thinner than that of the Ni coating, which indicates that the deposition rate is decreased significantly with the addition of PTFE particles into the Ni plating bath.

3.4. Microstructures

XRD patterns of the as-deposited coatings were measured and are given in Figure 7. Standard XRD reports for Ni (JCPDS 04-0850) and brass substrate (CuZn alloy: JCPDS 00-050-1333) are also

shown in this figure. The peaks at 44.5° , 51.8° , and 76.4° in Figure 7a are assigned to the face-centered cubic (fcc) Ni planes of (111), (200), and (220), respectively, according to the report of JCPDS 04-0850 [33,34].

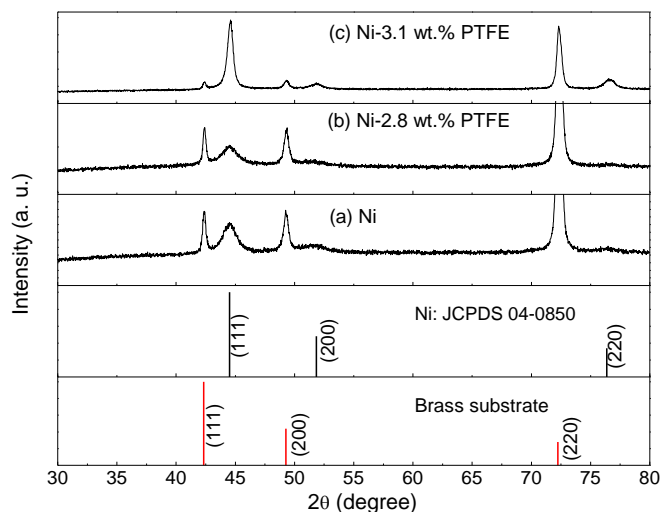


Figure 7. XRD patterns of the as-deposited Ni coating and Ni–PTFE composite coatings. Standard XRD reports for Ni (JCPDS 04-0850) and brass substrate (JCPDS 00-050-1333) are also shown in this figure.

For the Ni–2.8 wt.% PTFE composite coating electrodeposited from Ni–5PTFE electrolyte, XRD patterns (Figure 7b) are similar with that of the Ni coating, indicating that no obvious phase change occurs upon the introduction of 5 g l^{-1} PTFE particles in the plating bath. Both peaks of Ni (111) plane are relatively broad indicative of refined grain structure in the coatings, which is also evidenced by the SEM observations. Strangely, as shown in Figure 7c, the peak of Ni (111) plane for the Ni–3.1 wt.% PTFE composite coating becomes very sharper and the peak intensity ratio of the (111) to (200) diffractions is around 4.23, which is much higher than the value from a polycrystalline Ni with randomly distributed grains, 2.36 (according to JCPDS 04-0850). The present XRD result indicates that the {111} plane of the electrodeposited Ni–3.1 wt.% PTFE composite coating is preferentially oriented parallel to the surface of the supporting substrate [42], which should be consistent with the orientation and geometry of the as-deposited Ni–3.1 wt.% PTFE composite coating as illustrated in Figure 3e. The diffraction peaks corresponding to PTFE are not found in the XRD patterns of the synthesized coatings due to its small concentration (less than 5 wt.%).

3.5. Wettability and corrosion resistance

The surface wettability of the as-deposited coatings are studied by CA measurements, and the corresponding images of a water droplet of about $1 \mu\text{L}$ on the surface of the coatings are given in Figure 8. Figure 8a gives a CA value of $97 \pm 2^\circ$ for the pure Ni electrodeposited at room temperature.

The similar CA value was also reported in our previous study[34]. The Ni–2.8 wt% PTFE composite coating exhibits a relatively lower CA value ($91\pm 1^\circ$ as observed in Figure 8b) to that of the pure Ni coating, which should be attributed to its lower surface roughness as shown in Figure 5.

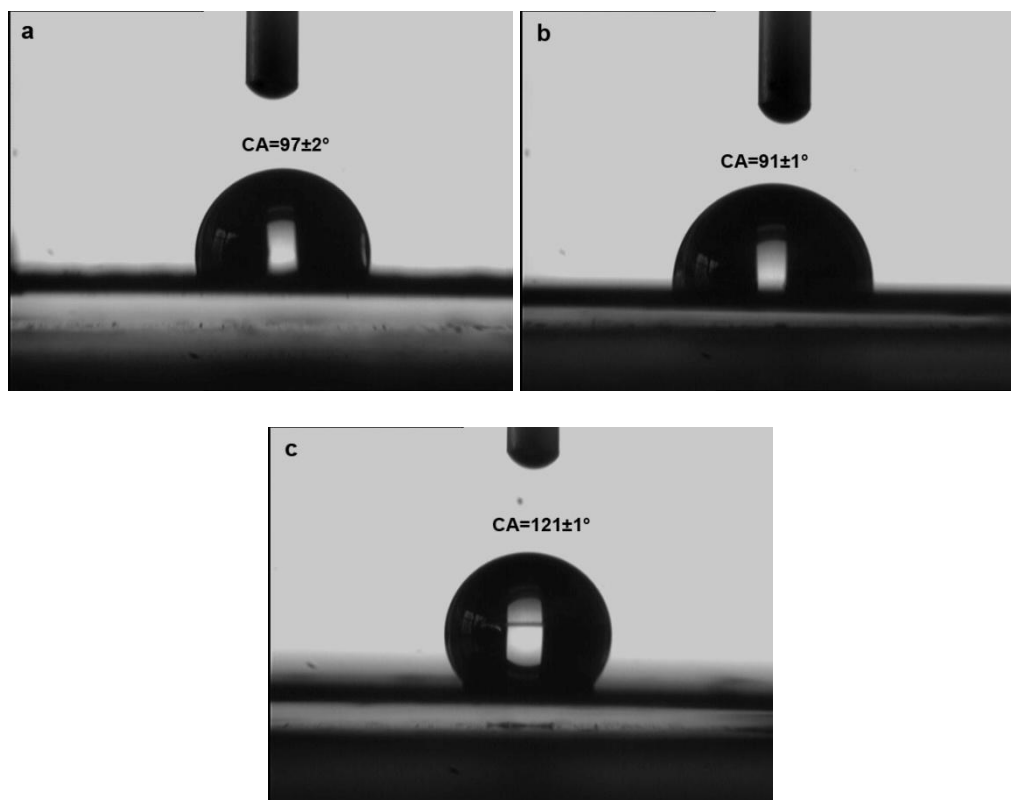


Figure 8. Contact angle measurements of a water droplet (1 μL) on the Ni coating (a); (b) Ni–2.8 wt.% PTFE, and (c) Ni–3.1 wt.% PTFE composite coatings.

Interestingly, the Ni–3.1 wt% PTFE composite coating exhibits a significant hydrophobic surface with a CA value of $121\pm 1^\circ$ which is also slightly higher than the CA value of water on a PTFE substrate (shown in Figure 1a). Hydrophobic surfaces generally share two common features: they are made of (or covered by) hydrophobic materials and the surfaces are not flat at the micro/nanometer scales but have micro/nanobinary structures [34]. Exceptionally, if the Ni coating was composed by vigorous nanoscaled structures with an appropriate surface roughness, the superhydrophobic Ni surface could also be obtained without any further modifications by low surface-energy materials[34]. Here, we suggest two possible reasons for the hydrophobicity of the Ni–3.1 wt% PTFE composite coating. One should be attributed to the vigorous nanoscaled structures on the coating surface as shown in Figure 3e, which is similar to that of the superhydrophobic Ni coating electrodeposited at a high temperature of 90°C [34]. The other might be related to the PTFE particles with lower surface-energy appeared on the Ni surface (see Figure 4). A higher CA value of the Ni–3.1 wt% PTFE composite coating over the PTFE substrate might be correlated with the synergistic effect of both the vigorous nanoscaled structure of the coating surface and the water repellency of PTFE.

The electrochemical anticorrosion behaviors of Ni and Ni-PTFE composite coatings were assessed by measuring the potentiodynamic polarization curves of the coated samples in a 3.0 wt.% NaCl aqueous solution.

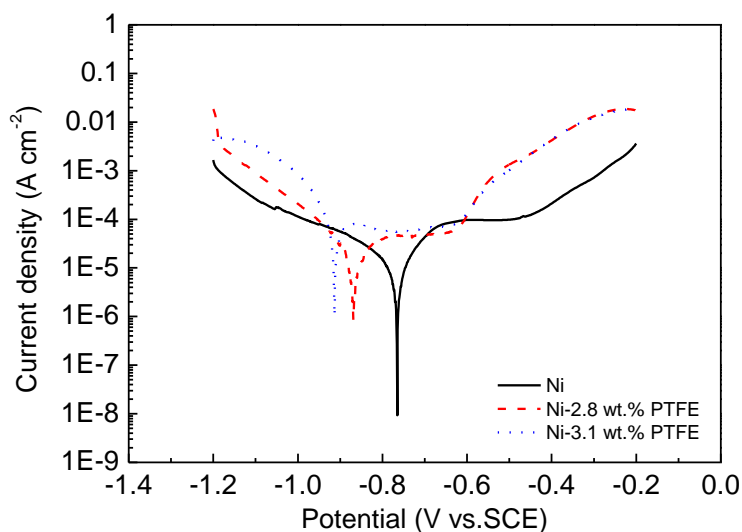


Figure 9. Electrochemical polarization curves of the electrodeposited Ni coating and Ni-PTFE composite coatings.

The derived polarization curves are presented in Figure 9. The cathodic reaction in the polarization curves corresponds to the evolution of the hydrogen. The anodic branch of polarization curve has the most important features related to the corrosion resistance.

Table 1. Corrosion potentials and current densities derived from the electrochemical measurements (Figure 9) of the coatings electrodeposited in this study.

Coatings	Corrosion potential, $E_{\text{corr}}/ \text{V}$	Corrosion current density, $i_{\text{corr}}/ \text{A cm}^{-2}$
Ni	-0.76	7.94×10^{-6}
Ni-2.8 wt.% PTFE	-0.86	9.04×10^{-6}
Ni-3.1 wt.% PTFE	-0.91	5.52×10^{-5}

Figure 9 shows that both pure Ni coating and Ni-PTFE composite coatings exhibit passivation region, which indicates that anodic reaction is inhibited to a great extent with the increase of anodic potential. It can be also seen from Figure 9 that compared with pure Ni coating, Ni-PTFE composite coatings exhibit lower passive corrosion current densities suggesting an excellent anticorrosion of the passive films observed in Ni-PTFE composite coatings. Corrosion potential (E_{corr}) and corrosion current density (i_{corr}) derived from the polarization curves in Figure 9 using Tafel extrapolation are summarized in Table 1. The pure Ni coating exhibits the noblest E_{corr} with a value of -0.76 V and the lowest i_{corr} with a value of $7.94 \times 10^{-6} \text{ A cm}^{-2}$ compared with the two Ni-PTFE composite coatings. For

the Ni–2.8 wt% PTFE and Ni–3.1 wt% PTFE composite coatings, the E_{corr} becomes more negative and the i_{corr} gets higher. This may be due to the incorporation of PTFE particles into the Ni matrix generating lots of micro-pores or active sites which are easily to be corroded. Moreover, as indicated in Table 1, the Ni–3.1 wt.% PTFE coating exhibits one order of magnitude higher corrosion current density over the pure Ni coating, which might be attributed to the inter-granular corrosion taking place at the crystal boundaries since addition of 10 g l⁻¹ PTFE results in highly sheet-like crystalline nature Ni in the deposit as discussed in the section of 3.4. The similar result was also reported in the Ni–PTFE coatings electrodeposited from the aqueous system by Tian et al [43].

3.6. Wear analysis

The friction coefficients of the as-deposited coatings against Si₃N₄ ball at a load of 1 N as a function of sliding cycle are shown in Figure 10 and the SEM images of the worn surface area are shown in Figure 11. For the Ni coating, the friction coefficient goes through two periods: running-in period with high friction coefficient and stable-state period with friction coefficient of about 0.75. For the Ni–2.8 wt% PTFE composite coating, the friction coefficient gets a little higher (0.83) than the Ni coating. The debris particles can be dragged along the surface in a wear test and therefore effect a higher friction coefficient as the test continues [38].

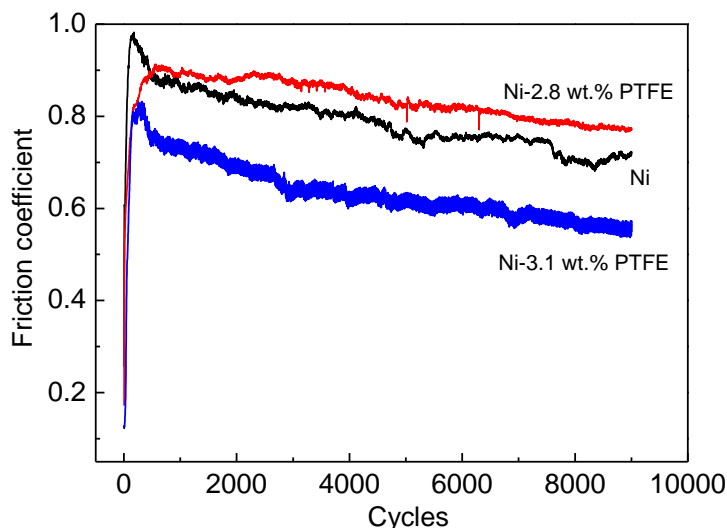


Figure 10. Plot of friction coefficient versus number of cycles for Ni coating and Ni–PTFE composite coatings.

However, for the Ni–3.1 wt% PTFE composite coating, the friction coefficient is about 0.60, much lower than the Ni coating, which might be due to the incorporation of PTFE particles and the different surface morphology as shown in Figure 3e. The corresponding SEM images of the worn surface area (Figure 11) further prove the above result. It is found that there is lots of debris on the surface of Ni–2.8 wt% PTFE composite coating and they are dragged along the surface. However, the

worn surface area of the Ni–3.1 wt% PTFE composite coating has less debris than the other two coatings.

The value of scratch volume reflects the wear resistance of the coatings and the width of the scratch trace is used to roughly estimate the scratch volume. The value of the scratch volume increases as the value of the scratch width increases. In this case, the value of scratch width was measured from the SEM images of the worn surfaces as shown in Figure 11. The width of the scratch of the Ni–2.8 wt.% PTFE and Ni–3.1 wt.% PTFE composite coatings is about 288 μm and 330 μm , respectively. Both of them are smaller than that of the Ni coating, 504 μm as shown in Figure 11, which indicates that the incorporation of PTFE particles into the Ni matrix effectively improves the wear resistance of the composite coatings.

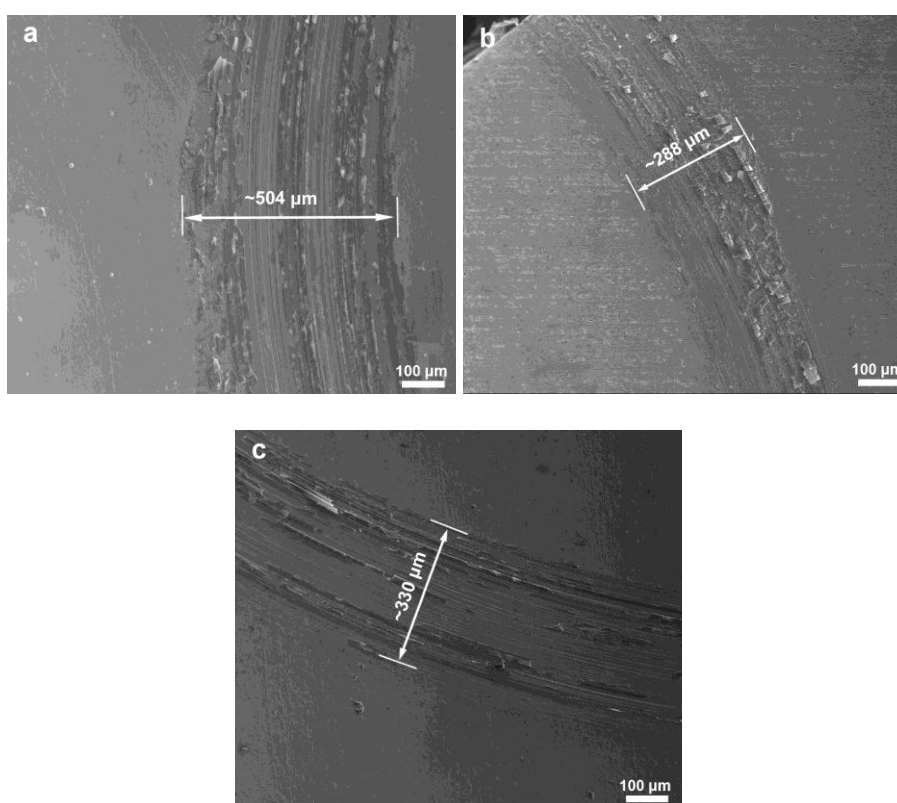


Figure 11. SEM micrographs of surfaces after wear tests. (a): Ni; (b): Ni–2.8 wt.% PTFE; and (c): Ni–3.1 wt.% PTFE.

4. CONCLUSION

Ni–PTFE composite coatings are facily electrodeposited from a simple solution of $\text{NiCl}_2 \cdot 6\text{H}_2\text{O}$ in the Ethaline with presence of PTFE particles. It should be noted that the proposed novel electrolyte is non-aqueous nature and the hydrophobic PTFE particles can be well dispersed in the electrolyte without the addition of wetting agents. SEM observations and EDS analysis indicate that the PTFE particles are successfully incorporated into the Ni matrix. The Ni–PTFE composite coatings

possess f.c.c. structures and have a preferred orientation growth along the (111) plane as the content of PTFE in the composite coatings increases. CA measurements show that the Ni–3.1 wt.% PTFE composite coating shows a hydrophobic behavior with CA values of about $121\pm 1^\circ$. The potentiodynamic polarization measurements indicate that the pure Ni exhibits the better anticorrosion behavior than the Ni–PTFE composite coatings. Furthermore, the more PTFE content the Ni–PTFE composite coatings have, the more negative corrosion potential and the higher corrosion current the coatings exhibit. It is also found that the Ni–PTFE composite coatings have a better wear resistance than the pure Ni coating due to the incorporation of PTFE. This study extends the synthetic route of Ni–PTFE composite coatings and further the application of the composite coatings.

ACKNOWLEDGMENTS

The work was supported by the National Natural Science Foundation of China (51001089, 51271169), the Specialized Research Fund for the Doctoral Program of Higher Education of China (20100101120026), and the Research Cooperation Project of Guangdong Province and the Ministry of Education (2010A090200047).

References

1. P. Rodrigo, M. Campo, B. Torres, M.D. Escalera, E. Otero and J. Rams, *Appl. Surf. Sci.*, 255 (2009) 9174
2. K. H. Hou and Y. C. Chen, *Appl. Surf. Sci.*, 257 (2011) 6340
3. M. Alishahi, S.M. Monirvaghefi, A. Saatchi and S.M. Hosseini, *Appl. Surf. Sci.*, 258 (2012) 2439
4. F. Wang, S. Arai and M. Endo, *Mater. Trans.*, 45 (2004) 1311
5. J. Wang, J. Tian, X. Liu, Y. Yin and X. Wang, *Thin Solid Films*, 519 (2011) 5905
6. Y. Suzuki, S. Arai and M. Endo, *J. Electrochem. Soc.*, 157 (2010) D50
7. S. Armini, C.M. Whelan, M. Moinpour and K. Maex, *J. Electrochem. Soc.*, 156 (2009) H18
8. W. Shao, D. Nabb, N. Renevier, I. Sherrington, Y. Fu and J. Luo, *J. Electrochem. Soc.*, 159 (2012) D671
9. A. Bund, and D. Thiemig, *Surf. Coat. Technol.*, 201 (2007) 7092
10. A.P. Abbott, K. El Ttaib, G. Frisch, K.J. McKenzie and K.S. Ryder, *Phys. Chem. Chem. Phys.*, 11 (2009) 4269
11. W. Wang, F.Y. Hou, H. Wang and H.T. Guo, *Scripta Mater.*, 53 (2005) 613
12. F. Hou, W. Wang and H. Guo, *Appl. Surf. Sci.*, 252 (2006) 3812
13. L. Shi, C. Sun, P. Gao, F. Zhou and W. Liu, *Appl. Surf. Sci.*, 252 (2006) 3591
14. A. Sohrabi, A. Dolati, M. Ghorbani, M.R. Barati and P. Stroeve, *J. Phys. Chem. C*, 116 (2012) 4105
15. S. Faraji, A. Rahim, N. Mohamed and C. Sipaut, *J. Coat. Technol. Res.*, 9 (2012) 115
16. N.K. Shrestha, I. Miwa, and T. Saji, *J. Electrochem. Soc.*, 148 (2001) C106
17. D.K. Singh and V.B. Singh, *J. Electrochem. Soc.*, 158 (2011) D114
18. A. Ramalho and J.C. Miranda, *Wear*, 259 (2005) 828
19. I.R. Mafi and C. Dehghanian, *Appl. Surf. Sci.*, 257 (2011) 8653
20. M. Mohammadi and M. Ghorbani, *J. Coat. Technol. Res.*, 8 (2011) 527
21. K. Pan and C. Fu, *J. Micromech. Microeng.*, 20 (2010) 095020
22. M. Rezrazi, M.L. Doche, P. Berçot, J.Y. Hihn, *Surf. Coat. Technol.*, 192 (2005) 124
23. Q. Zhao, Y. Liu and E.W. Abel, *Mater. Chem. Phys.*, 87 (2004) 332

24. R. Balaji, M. Pushpavanam, K.Y. Kumar and K. Subramanian, *Surf. Coat. Technol.*, 201 (2006) 3205
25. J.D. Miller, S. Veeramasuneni, J. Drelich, M.R. Yalamanchili and G. Yamauchi, *Polym. Eng. Sci.*, 36 (1996) 1849
26. H. Matsuda, Y. Kiyono, M. Nishira and O. Takano, *Trans. I M. F.*, 72 (1994) 55
27. H. Matsuda, M. Nishira, Y. Kiyono and O. Takano, *Trans. I. M. F.*, 73 (1995) 16
28. Q. Zhao, Y. Liu, H. Müller-Steinhagen and G. Liu, *Surf. Coat. Technol.*, 155 (2002) 279
29. M. Armand, F. Endres, D.R. MacFarlane, H. Ohno and B. Scrosati, *Nat.Mater.*, 8 (2009) 621
30. F. Endres, *Chem.phys.chem.*, 3 (2002) 144
31. A.P. Abbott, D. Boothby, G. Capper, D.L. Davies and R.K. Rasheed, *J. Am. Chem. Soc.*, 126 (2004) 9142
32. C.D. Gu, X.J. Xu and J.P. Tu, *J. Phys. Chem. C*, 114 (2010) 13614
33. C.D. Gu, Y.H. You, Y.L. Yu, S.X. Qu and J.P. Tu, *Surf. Coat. Technol.*, 205 (2011) 4928
34. C.D. Gu and J. Tu, *Langmuir*, 27 (2011) 10132
35. C.D. Gu, Y.J. Mai, J.P. Zhou, Y.H. You and J.P. Tu, *J. Power Sources*, 214 (2012) 200
36. Y.H. You, C.D. Gu, X.L. Wang and J.P. Tu, *Surf. Coat. Technol.*, 206 (2012) 3632
37. Y.H. You, C.D. Gu, X. Wang and J. Tu, *J. Electrochem. Soc.*, 159 (2012) D642
38. A.P. Abbott, K. El Ttaib, G. Frisch, K.S. Ryder and D. Weston, *Phys. Chem. Chem. Phys.*, 14 (2012) 2443
39. K.E. ttaib, *The Electrodeposition of Composite Materials using Deep Eutectic Solvents*, PhD Thesis, University of Leicester, 2010, pp. 118
40. A.P. Abbott, K.S. Ryder and U. Konig, *Trans. I. M. F.*, 86 (2008) 196
41. F.R. Bento and L.H. Mascaro, *Surf. Coat. Technol.*, 201 (2006) 1752
42. C.D. Gu, Y.H. You, X. L. Wang and J. P. Tu, *Surf. Coat. Technol.*, 209 (2012) 117
43. J.T. Tian, X.Z. Liu, J.F. Wang, X. Wang and Y.S. Yin, *Mater. Chem. Phys.*, 124 (2010) 751